

# Investigation of neutronic parameters of $^{nat}\text{U}$ spallation target irradiated by low-energy protons

Zohreh Gholamzadeh<sup>1</sup> · Seyed Mohammad Mirvakili<sup>1</sup> · Amin Davari<sup>1</sup> · Mostafa Hassanzadeh<sup>1</sup>

Received: 11 September 2015 / Revised: 15 November 2015 / Accepted: 22 November 2015 / Published online: 13 July 2016  
© Shanghai Institute of Applied Physics, Chinese Academy of Sciences, Chinese Nuclear Society, Science Press China and Springer Science+Business Media Singapore 2016

**Abstract** Accelerator-based neutron sources could outstandingly compete with the reactor-based ones, which are widely used for research aims and radioisotope production. Spallation neutron sources are used by many research centers. In this work, the potential of natural uranium spallation target irradiated by low-energy protons for production of an external neutron source was investigated. MCNPX code was used to model the spallation target. The results showed using 30-MeV protons of 100  $\mu\text{A}$  current a neutron flux in order of  $10^7$  n/s·cm<sup>2</sup> leaks from an optimized-dimension target. Different physical models available in the computational code do not result in significant relative discrepancies for neutron yield and deposited heat calculations. Water with a velocity of 0.6 m/s can be used as coolant for the spallation target to keep the surface temperature under 100 °C at atmospheric pressure.

**Keywords**  $^{nat}\text{U}$  target · Spallation · Neutronic parameters · MCNPX 2.6.0 code

## 1 Introduction

Spallation process is a key reaction, which creates spallation neutrons in target material irradiated by charged particles. In the first stage, the primary incident particle reacts with nucleons (neutrons and protons) inside the nucleus. The reactions that follow create an intranuclear

cascade of high-energy ( $>20$  MeV) protons, neutrons and pions within the nucleus. During the intranuclear cascade, some of these energetic hadrons escape as secondary particles. Others deposit their kinetic energy in the nucleus, leaving it in an excited state. In the second stage (nuclear de-excitation), evaporation takes place when the excited nucleus relaxes by emitting low-energy ( $<20$  MeV) neutrons, protons, alpha particles, etc., with the majority of the particles being neutrons. The low-energy neutrons produced during nuclear de-excitation are important in the spallation source because they can be moderated (reduced) to even lower energies for use as research probes. After evaporation, the nucleus that remains may be radioactive and may emit gamma rays [1].

Different target materials could be used as spallation target of which heavier targets are considered as the best. The uranium target could have some attractions as a neutron source than conventional lead–bismuth (PbBi) due to its stunningly higher spallation neutron yield. Many experimental and theoretical studies have been performed on bare uranium spallation target to evaluate its neutron production capability and the mechanism of the spallation process in a wide range of incident proton energy. In the following, some of them will be reviewed.

Ismailov et al. [2] carried out the feasibility study of natural uranium spallation target in order to improve the neutron balance in the accelerator-driven system (ADS) of Japan Atomic Energy Agency (JAEA) type to transmute minor actinide (MA). In this respect, the comparative study of uranium target with conventional PbBi both in bare case and in ADS was implemented. In addition, pin-type uranium target cooled by PbBi was introduced aiming at enhancing the spallation target properties such as neutron generation efficiency and operation temperature. They used MCNPX

✉ Zohreh Gholamzadeh  
cadmium\_109@yahoo.com

<sup>1</sup> Reactor Research School, Nuclear Science and Technology Research Institute, Tehran, Iran

2.7.c to determine neutronics of the modeled spallation target. First, they studied bare cylindrical spallation target without a blanket. The neutron yield depending on target size was investigated for determining the optimal conditions of the effective neutron source. They optimized the target length at fixed proton beam energy equal to 1.5 GeV with beam radius of 1 cm. Their results showed the irradiated optimized-dimension target could produce about 65 n/p.

Hashemi-Nezhad et al. [4] studied experimental target setup made of four cylindrical lead targets each with diameter 8.4 cm and length 11.4 cm where a natural uranium blanket surrounds each of the four target sections. Each uranium blanket is composed of 30 uranium rods of diameter 3.6 cm (including the Al cladding) and length 10.4 cm hermetically sealed in aluminum cladding. The uranium rods are arranged in the form of hexagonal (triangular) lattice with the pitch size of 3.6 cm. The weight of natural uranium in each blanket section is 51.6 kg, and the whole setup contains a total of 206.4 kg of natural uranium. In this work, they used MCNPX 2.6.c to study neutronic performance of the irradiated target and the target size was fixed at constant for each proton beam energy, while in the proton energy higher than 1.5 GeV the optimal target length should be longer than 50 for uranium target. The radius of the proton beam was kept constant at 1 cm, and the neutron yield at proton energies in range starting from 500 MeV up to 2 GeV was simulated with the used code. Their results show that proton-, pion- and photon-induced fissions contribute significantly to the total fission rate in the samples within the target volume and its immediate vicinity, while about 97 % of fissions come from (*n,f*). Another obtained result from them indicates that the code prediction of the fission rate is consistently lower by  $22 \pm 0.14$  % than the experimental value for the fission foils placed in the blanket region when Bertini and RAL models are used in the calculations. This deviation reduces to  $13 \pm 0.09$  % when the Bertini and Abla models or CEM03 model is used instead [3].

Hashemi-Nezhad et al. [4] investigated variation of the escaping, captured and total neutron yield as a function of the target radius in irradiation of range-long targets of  $^{nat}\text{W}$ ,  $^{nat}\text{Pb}$ ,  $^{232}\text{Th}$  and  $^{238}\text{U}$  with 1.0-GeV protons. They used MCNPX 2.7.c code to study the selected targets. Their result showed a 10 cm radius presents peak of escaped neutron yield, and the target radius enhancement more than 10 cm is not efficient [4].

Sahin et al. [5] demonstrated that the heavier target nucleus and the higher incident proton energy resulted in a greater number of neutrons which would emanate from the target nucleus so that thorium and uranium targets will generate more neutrons than lead and bismuth. Their study analyzes the integral  $^{233}\text{U}$  and  $^{239}\text{Pu}$  breeding rates, neutron multiplication ratio through (*n,xn*) and fission reactions,

heat release, energy multiplication and consequently the energy gain factor in infinite size thorium and uranium as breeder material in an accelerator-driven systems (ADS) irradiated by a 1-GeV proton source [5].

The literature shows such evaluations have started from the 1970s, and some experiments were carried out on uranium target to study the spallation process inside it as well as its neutronic behavior. The following review illustrates them briefly.

Russell et al. [6] irradiated depleted-uranium target by 800 MeV to understand proton spallation reactions which are important to the spallation neutron source development [6]. Vasilkov et al. (1978) investigated neutron multiplication in massive metal uranium targets bombarded by 300-, 400-, 500- and 660-MeV protons. The total mass of every rectangular target with dimension of  $56 \times 56 \times 64$  cm was 3.5 ton [7].

Whereas the uranium spallation target is of interest because of its high-neutron yield, investigation of neutronic parameters of natural uranium target irradiated using different proton energies was proposed in this work.

## 2 Materials and methods

MCNPX 2.6.0 code [8] was used to model the spallation process in a cylindrical natural uranium target. To investigate the effect of proton energy enhancement on fission rate growth inside the spallation target, a fixed dimension of  $10 \times 10$  cm was chosen for the cylindrical target and 30-, 50-, 70- and 90-MeV proton energies were used to induce spallation in the modeled target separately.

As the de Broglie wavelength of the incident proton is around a nucleon dimension ( $\sim 1.7$  fm), it interacts with individual nucleons in the target nucleus (instead of creating a compound nucleus). The projectile shares its kinetic energy with target nucleons by elastic collisions, and a cascade of nucleon–nucleon collisions proceeds. However, it is said intranuclear cascade (INC) is more probable for proton energies of  $>100$  MeV, but its occurrence is probable for low energies also [9].

According to the following equation, the de Broglie wavelength [10] of a 30-MeV incident proton is  $\sim 5.22$  fm.

$$\lambda = \frac{hc}{\sqrt{2m_0p c^2 E_p}} (fm) \quad (1)$$

where  $hc = 197.32$  (MeV·fm), proton rest mass is 938 MeV, and  $E_p$  is incident proton energy. It should be mentioned that uranium target diameter is 15.49 fm. Hence, an INC can be applied reasonably well to study the systematics of the propagation of nucleons at low energies of a few tens of MeV [11]. Therefore, a 30-MeV proton could interact with a uranium target by intranuclear cascade (INC).

First, the cylindrical target dimension was optimized at the selected proton energies. An optimized radius was chosen so that there is not more than ~5 % enhancement in escaped neutron yield from the spallation target when it is getting bulkier. A void sphere was considered around the cylindrical target, and the escaped neutrons were tallied over the spherical surface. The same procedure was used to determine an optimized target length of the fixed-radius target at any incident proton energy. Neutron spectra leaked from the optimized-dimension spallation target were determined for any proposed projectile energy. Different physical models of MCNPX code, including Bertini/Drenser, Bertini/Abla, Isabel/Drenser, Isabel/Abla, INCL4/Drenser, INCL4/Abla and CEM, were used to calculate neutron yield, deposited energy and mass distribution of different isotopes, which are produced inside the modeled optimized-dimension uranium spallation target. An obtained relative discrepancy between the results using different physical models was discussed.

The modeled targets were irradiated by proton beam with a current of 100  $\mu$ A (5 mm spatial FWHM). Many particles (2,000,000) were transported to reduce the calculation errors to <0.4 %. The <sup>239</sup>Pu production rate in any optimized target was discussed. Fission per absorption ratio was determined for any optimized spallation target.

Water coolant was proposed to cool the 30-MeV proton-induced one with a specific velocity. The target temperature profile was obtained using FLUENT code. Impacts of high-energy proton projectile on leaked neutron yield and deposited heat inside the uranium target with a fixed dimension were discussed.

ENDF/B-VI continuous-energy cross sections were used for the calculations. Target temperature enhancement effects on the escaped neutron yield, the deposited heat and the leaked neutron flux from the optimized-dimension target were determined using TMP card and temperature-related cross section libraries of .70c, and .71c from endf70 library of the used code.

Delay gamma weights on the escaped neutron yield were ignored for the low-energy investigations. It is mandatory for high-energy applications and could be applied by the ACT card ability of MCNPX2.7 code.

To determine neutron spectra in latter surface of the spallation system, F1 tally can be employed in which each time a particle crosses the specified surface, its weight is added to the tally, and the sum of the weights is reported as the F1 tally in the MCNP output [12].

In the energy range, where nuclear data tables are available, the neutron, photon and proton energy depositions are determined using the heating numbers from the nuclear data tables. These heating numbers are estimates of the energy deposited per unit track length. In addition, the  $dE/dx$  ionization contribution for electrons and/or protons is added for MODE E or MODE H.

Above the tabular energy limits or when no tabular data are available, energy deposition is determined by adding different factors. For charged particles, ionization ( $dE/dx$ ) energy is deposited uniformly along the track length (which is an important factor when creating mesh tallies). All other energy depositions are calculated at the time of a nuclear interaction. The energy of secondary particles, if they are not to be tracked (i.e., not included on the MODE card), will be deposited at the point of the interaction. Nuclear recoil energy will be deposited at the point of interaction too, unless heavy ion transport is specified. In order to obtain the most accurate energy deposition tallies, the user must contemplate or consider all potential secondary particles on the MODE card. PEDEP card can be used to calculate energy deposition [8]. The tally computes the energy deposition using Eq. 2 [13]:

$$F_6 = \frac{\rho_a}{\rho_g} \int_v \int_t \int_E H(E) \Phi(r, E, t) dE dt \frac{dV}{V} \left( \frac{\text{MeV}}{g(\text{Source particle})} \right) \quad (2)$$

where  $\rho_a$  is atom density (atoms/barn-cm),  $\rho_g$  is gram density ( $g/cm^3$ ), and  $H(E)$  is heating response (added over nuclides in a material). F6 tally for neutrons is calculated via:

$$H(E) = \sigma_T(E) H_{ave}(E) \quad (3)$$

where

$$H_{ave}(E) = E - \sum_i P_i(E) [\bar{E}_{out}(E) - Q_i + \bar{E}_{\gamma i}(E)] \quad (4)$$

and  $\sigma_T$  = total neutron cross section,  $E$  = incident neutron energy,  $P_i(E)$  = probability of reaction  $i$ ,  $E_{out}$  = average exiting neutron energy for reaction  $i$ ,  $Q_i$  =  $Q$  value of reaction  $i$ ,  $E_{\gamma i}$  = average energy of exiting gammas for reaction  $i$ .

$F_6$  tally for photons is calculated via the following equations:

$$H(E) = \sigma_T(E) H_{ave}(E) \quad (5)$$

$$H_{ave}(E) = \sum_{i=1}^3 P_i(E) \times (E - \bar{E}_{out}) \quad (6)$$

$i = 1$  incoherent (Compton) scattering with form factors,  $i = 2$  pair production,  $i = 3$  photoelectric [13].

RES card of MCNPX is used to calculate residual nuclei inside the irradiated spallation target [8].

### 3 Results and discussion

Neutron yield and deposited heat were calculated in the modeled uranium spallation target. At the first stage, a 10 cm fixed height was considered for the target and an

optimized target radius was determined. The calculations showed that for the target irradiated by 30-MeV protons, a 5 cm radius is adequate, whereas the target radius enhancement will not increase the escaped neutron yield more than 5 %. Therefore, a fixed 5 cm radius was used for the target and its efficient height was determined. The results display that after 10 cm height, the target elongation does not improve the obtained neutron yield significantly. Hence, the optimized cylindrical target dimension at proton irradiation of 30 MeV was selected as  $10 \times 10$  cm (Fig. 1).

The same procedure was followed to determine an optimized target dimension for irradiations by 50-, 70- and 90-MeV protons. The computational results showed a  $10 \times 10$  cm dimension is the best for irradiation by 50-MeV protons and bigger dimensions not only don't increase the leaked neutron yield more than 5 % but also more massive uranium spallation targets are in less interest due to higher residual nuclei production and thermo-hydraulic point of views (Fig. 2).

According to Figs. 3 and 4, the best dimension for 70- and 90-MeV irradiations was chosen as  $8 \times 10$  cm.

Default physical model (Bertini/Drenser) of MCNPX code was used for previous calculations. At the next stage, the impact of the code available physical models on such calculations for the optimized dimensions will be discussed. By using two LCA and LEA cards, the different physical models could be applied (Table 1).

Relative discrepancy of neutron yield and deposited heat values calculated by different INC physical models of MCNPX code was investigated at the proposed proton energy. The results indicated at 30-MeV proton energy, there is no significant relative discrepancy ( $<4$  % on average) between neutron yield values calculated by the INCL4 and Bertini models. About 19 % of relative discrepancy is seen between Isabel/Drenser and CEM model. In case of heat deposition inside the modeled target is seen, an average relative discrepancy of  $<0.035$  % occurs between INC models which use

Drenser de-excitation models. A similar behavior is seen in the obtained data from Abl de-excitation model. CEM presents a heating value close to INC models with Abl de-excitation model. In case of the heating value calculation, about 0.7 % relative discrepancy is seen between INCL4/Drenser (maximum) and INCL4/Abl (minimum) (Fig. 5).

Projectile energy enhancement resulted in average higher discrepancies of spallation neutron yield and deposited heat values (0.04–5.3 and 3.16–23 %, respectively, correspond to 30- and 90-MeV proton energy) obtained by different physical models (Figs. 6, 7 and 8).

The CEM model presented the highest neutron yield values at all investigated projectile energies, while Isabel/Drenser resulted in the least values. Overall, the MCNPX code allows the user to choose between intranuclear cascade and fission-evaporation model combinations among Isabel, Bertini and INCL4 for cascade and Drenser (associated with RAL or ORNL fission models) and Abl for de-excitation. Whereas most portion of neutron yield is related to INC stage, Isabel/Abl and Isabel/Drenser models showed close neutron yield values at all the investigated proton energies. The same behavior is seen about Bertini and INCL4 models. In case of the deposited heat, which is mainly related to the fission-evaporation stage, Drenser model data are close to each other. The same behavior is seen in the case of Abl model at all investigated projectile energies. As it is observed from Figs. 6, 7 and 8, Drenser model resulted in the highest deposited heat values.

Different researches show that INCL4/Abl or Isabel/Abl physics models can obtain very reasonable predictions of spallation–fission products in uranium target [14, 15]. Hence, CEM/INCL4/Abl and Isabel/Abl models were used to calculate the mass distribution of the produced isotopes inside the irradiated uranium target. Two options of RES card and histp proficiency of the used computational code could be applied to calculate mass distribution of the produced residual nuclei inside the irradiated target. If histp proficiency is used for the

**Fig. 1** Neutron spallation yield dependence on **a** radius, **b** height, proton energy: 30 MeV

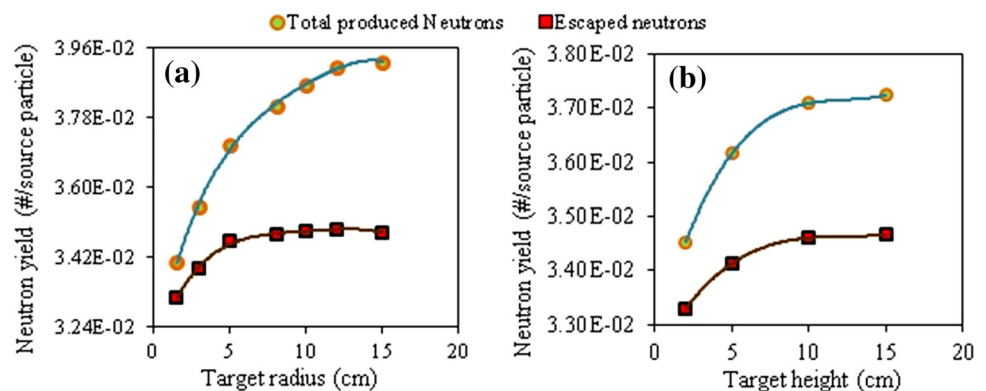


**Fig. 2** Neutron spallation yield dependence on **a** radius, **b** height, proton energy: 50 MeV

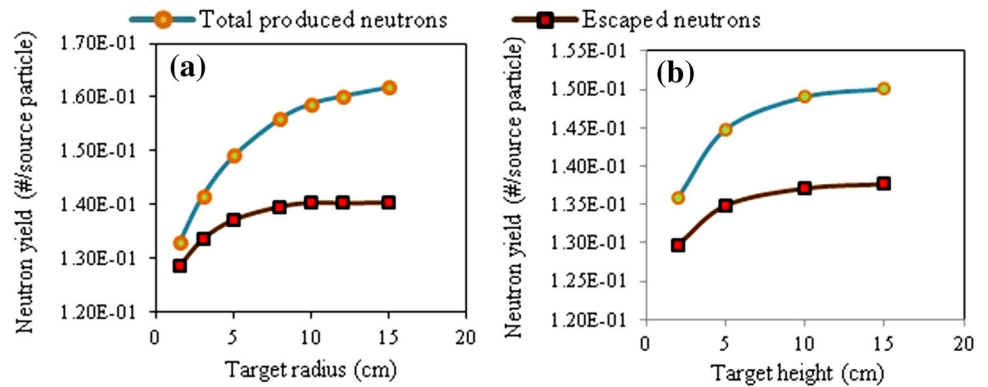


**Fig. 3** Neutron spallation yield dependence on **a** radius, **b** height, proton energy: 70 MeV

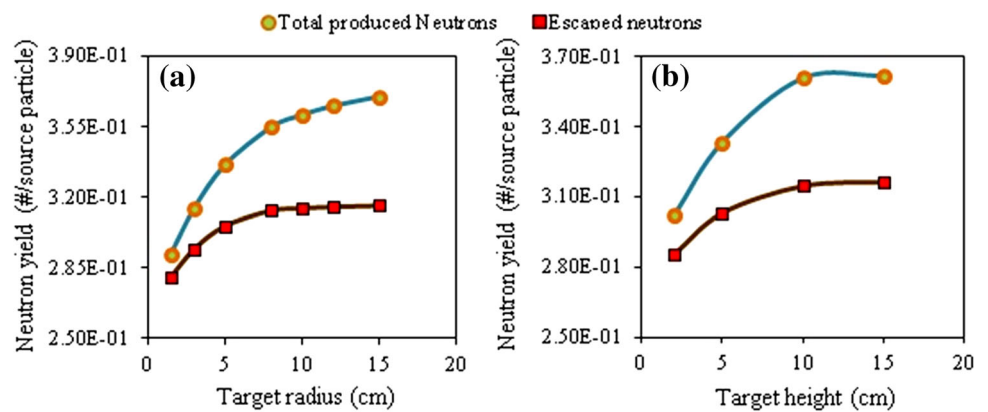
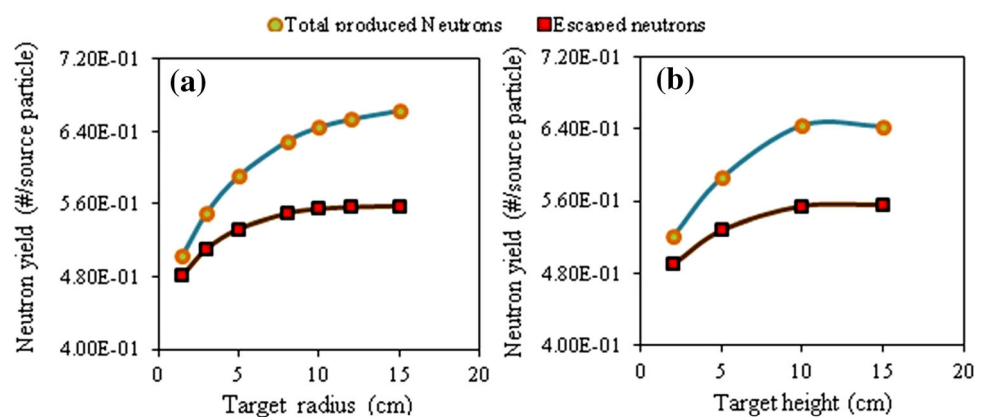


**Fig. 4** Neutron spallation yield dependence on **a** radius, **b** height, proton energy: 90 MeV



mentioned aim, the constructed file should be converted into a readable file by HTAPE3X.exe and IOPT 8 option.

The computational data showed CEM model data are underestimated in fission section of the mass distribution curve than the INCL4 and Isabel models. In addition, these two models present fitter data with each other (Fig. 9).

As shown in Fig. 9b, proton energy enhancement increases residual nuclei yield. For instance, the produced yield of  $A = 135$  becomes 3.13 times by proton energy enhancement of 30–50 MeV. Nevertheless, the yield

growth is happening slower between 50–70 and 70–90 MeV (1.90 and 1.60 times, respectively).

Calculation of neutron spectra leaked from the bare spallation targets shows 30-MeV proton injection with current of 100  $\mu\text{A}$  through the modeled uranium target produces a neutron flux in order of  $10^7$  n/s $\cdot\text{cm}^2$ . Using 50-MeV projectiles, the neutron flux becomes  $\sim 65$  times in comparison with 30-MeV proton projectiles. According to Fig. 10, higher energy projectiles do not increase the leaked neutron flux noticeably (3.85 and 2.85 times correspond to 70 and 90 MeV energy, respectively).

**Table 1** Different physical modes available in MCNPX code

Physical model	LCA	LEA
Isabel/Drenser	2j 2 5j 0	6j 0 j
Bertini/Abla	2j 1 5j 0	6j 2 j
Isabel/Abla	2j 2 5j 0	6j 2 j
CEM	2j j 5j 1	6j j j
INCL4/Drenser	2j 0 5j 2	6j 0 j
INCL4/Abla	2j 0 5j 2	6j 2 j

According to Table 2, the bare investigated spallation targets produce about 70 % neutrons with an energy range from 10 keV to 2 MeV. Irradiation of the targets by 100  $\mu$ A proton current produces a thermal power of 3.03–9.67 kW depending on the energy of an injected proton. Calculations showed the investigated targets produce 3.12–3.30 neutron per fission during irradiation. Malyshkin et al. [18] investigated the number of neutrons per fission in an 8  $\times$  12 cm cylindrical <sup>nat</sup>U target exposed by 600-MeV protons. They used Geant4-based code

**Fig. 5** **a** Neutron spallation yield, **b** deposited heat dependence on different INC physical models, proton energy: 30 MeV

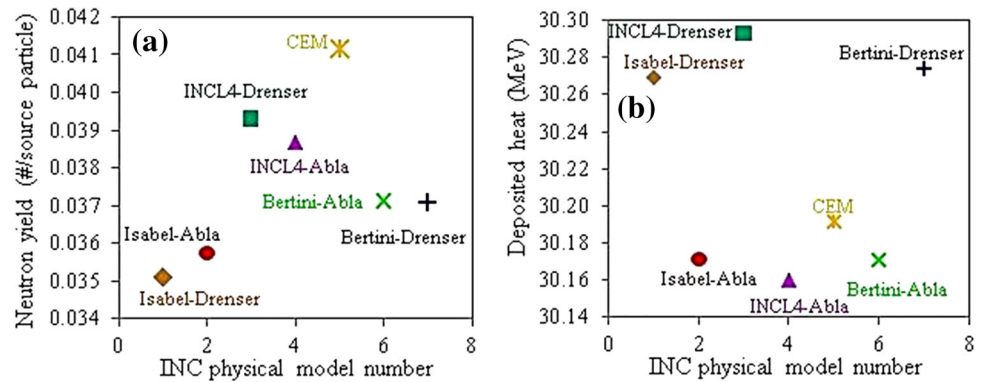


**Fig. 6** **a** Neutron spallation yield, **b** deposited heat dependence on different INC physical models, proton energy: 50 MeV

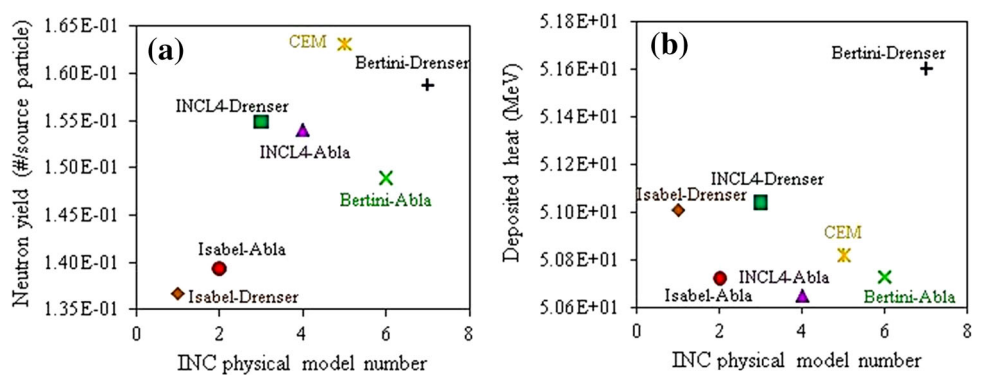


**Fig. 7** **a** Neutron spallation yield, **b** deposited heat dependence on different INC physical models, proton energy: 70 MeV

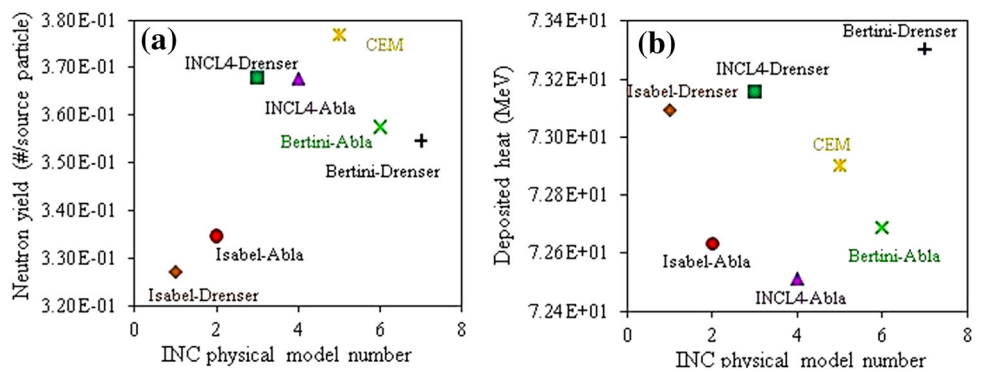


**Fig. 8** **a** Neutron spallation yield, **b** deposited heat dependence on different INC physical models, proton energy: 90 MeV

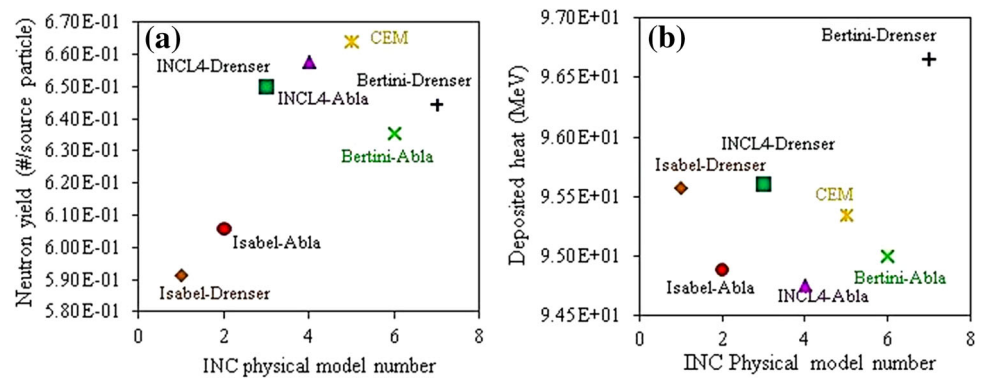


**Fig. 9** **a** Residual nuclei distribution, proton energy: 30 MeV, **b** residual nuclei distribution, Isabel/Abla model

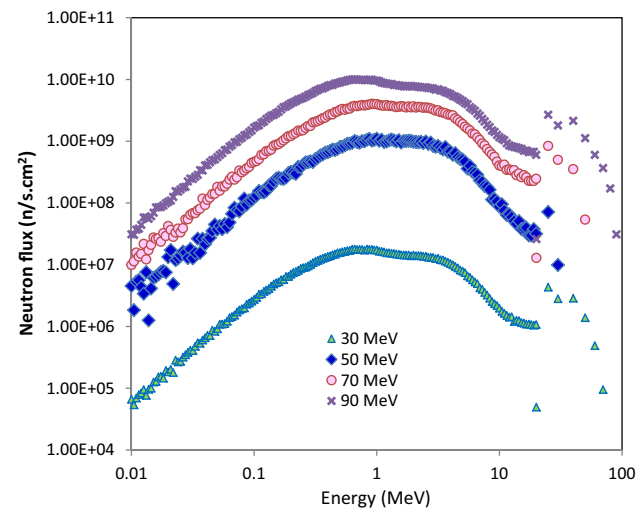
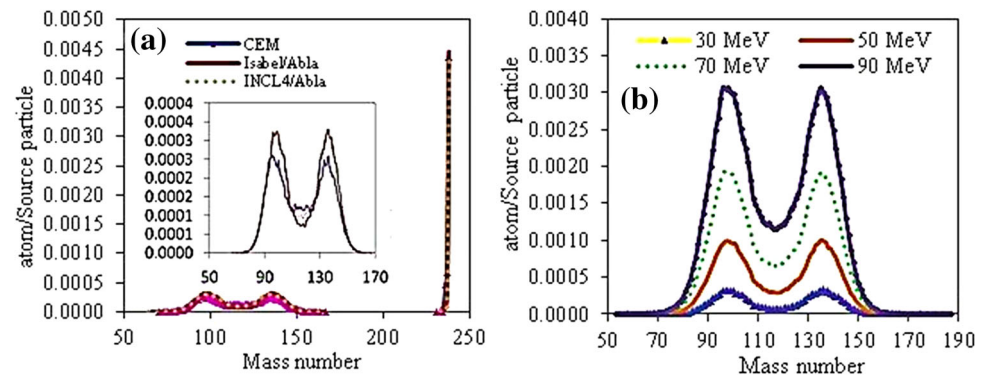


**Fig. 10** Neutron spectra leaked from the optimized bare spallation targets using different proton energies, Isabel/Abla model

MCADS for this calculation. Their obtained value (2.74) has about 14 % relative discrepancy with our data [18]. The natural uranium target experiences high fission per absorption ratio obviously because a hard neutron spectrum is available inside the spallation target and proton-fission reaction rate increases the fission rate. Application of higher proton energies will not increase the ratio because

the peak of proton-fission cross sections in natural uranium target happens around 50 MeV (Fig. 11).

As shown in Fig. 12, application of higher proton energy has the advantage of higher neutron yield productions from other reactions except fission. This noticeably higher ( $p, nx$ ) cross sections in comparison with fission at high proton energies eliminates the uranium target overheating and raises the neutron yield of the used spallation target.

Argonne research center used  $^{238}\text{U}$  target material irradiated by 450-MeV protons with 15  $\mu\text{A}$  current. They used eight disks of the mentioned material, and the designed spallation target bears 8 kW of thermal power. Light water was used as coolant of the spallation target. The coolant flow was 0.45 m/s, and its outlet temperature was  $<85^\circ\text{C}$ . In addition, 304 SS was used as target housing vessel and the hydraulic pressure differential across the target assembly is 1.0 bar, 15 psi [16].

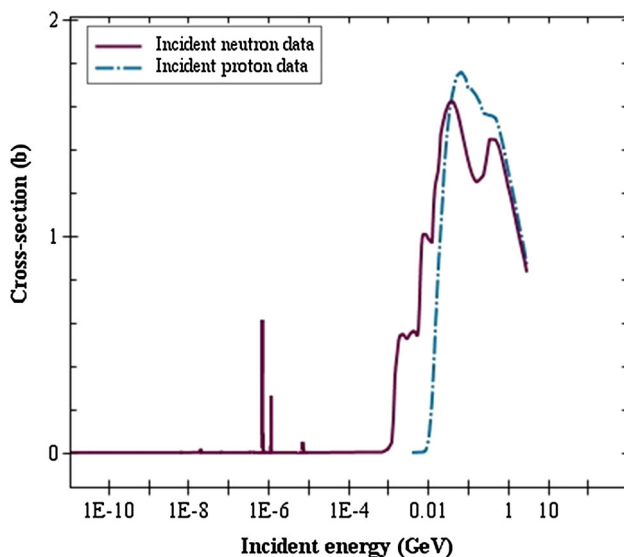
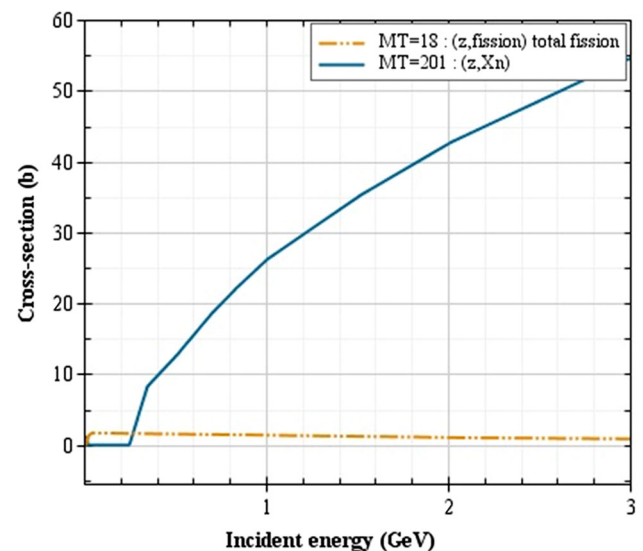
At Rutherford Appleton Laboratory, 800-MeV protons with a  $\sim 100 \mu\text{A}$  current induce the spallation process in a uranium target [17].

Calculations of this work show that the hottest section of the modeled targets is the proton beam entrance adjacent segments (because the Bragg peak of 30-MeV protons is occurring near to this location). According to Fig. 13, upper surface of the cylindrical target irradiated by

**Table 2**  $^{238}\text{U}$  target physical and neutronic specifications

Proton energy	30 MeV	50 MeV	70 MeV	90 MeV
Fraction of $E_n < 2$ MeV inside the target (%)	73.06	74.11	78.29	77.61
Fraction of $2 < E_n < 20$ MeV inside the target (%)	26.89	24.54	20.27	20.38
Fraction of $E_n < 2$ MeV leaked from the target (%)	70.22	66.68	67.95	70.15
Optimized dimension of the cylindrical target (cm)	$10 \times 10$	$10 \times 10$	$16 \times 10$	$16 \times 10$
Target mass (kg)	14.522	14.522	37.177	37.177
$^{235}\text{U}$ (g)	101.654	101.654	260.239	260.239
Fission per absorption ratio	2.57	2.80	2.11	2.12
Neutron per fission	3.12	3.30	3.30	3.29
$^{239}\text{Pu}$ buildup after 6 months (mg)	28.5	118.2	489.3	923.5
Deposited power (kW)	3.03	5.16	7.37	9.67
Accelerator beam power (kW)	3.0	5.0	7.0	9.0

All the calculations' errors were  $<0.4\%$  using a large particle history transport in the input file of the used computational code

**Fig. 11** Proton-fission and neutron-fission cross sections in  $^{238}\text{U}$  target, library: JENDL/HE2007**Fig. 12** Proton-fission and proton-nx cross sections in  $^{238}\text{U}$  target, library: JENDL/HE2007

30-MeV protons with 100  $\mu\text{A}$  current bears the most heat deposition. The target cooling by light water with a flow of 0.6 m/s will result in maximum temperature of 95  $^{\circ}\text{C}$  near to beam entry (Fig. 14).

The obtained calculations showed the target surface temperature remains under boiling temperature of water coolant to avoid the coolant boiling. Higher temperatures are experienced by internal sections, but the target surface keeps the temperature limitations.

Temperature-related cross sections were used for the optimized spallation target exposed of 30-MeV protons. The obtained results showed the escaped neutron yield of the modeled bare target decreased  $<0.02\%$  at higher temperature (598 K). However, resonance broadening is happening for the natural uranium target because of

temperature enhancement, but the inexistence of thermal and epithermal neutrons inside the modeled spallation target causes an approximately unchanged outgoing neutron flux. When water coolant covers the target, the mentioned value decreased  $<0.5\%$ . In sum up, temperature enhancement decreases the neutron flux around the spallation target somehow.

In MCNPX, net neutron production is tallied implicitly and is provided by default in the problem summary for neutrons. The problem summary shows net neutron production resulting from nuclear interactions (the component that accounts for neutron production by all particles transported using INC/pre-equilibrium/evaporation physics) and net production by  $(n,xn)$  reactions (neutrons created in inelastic nuclear interactions by neutrons below the



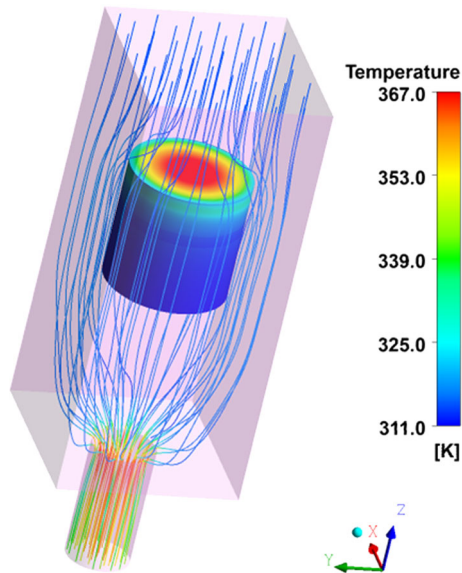


**Fig. 13** Temperature profile of the irradiated uranium target, proton energy: 30 MeV, current: 100  $\mu$ A

transition energy using evaluated nuclear data) [8]. Fraction of any reaction inside the optimized uranium target irradiated by 30-MeV protons is shown in Table 3. As is

seen, the produced neutrons by the INC, fast neutron fission, proton fission and  $(n, nx)$  are not depending on water coolant presence or neutron spectra softening as a result of the moderating role of the used coolant. Obviously, neutron-fission rate increases using the coolant because the number of neutrons with  $E_n < 2$  MeV increases.

Water coolant application increased the neutron flux leaked from the investigated target with a factor of 2.3.

Clearly, higher proton energies or currents produce higher deposited heat inside the uranium spallation targets, so that water could not be used as an adequate coolant at atmospheric pressure.

Higher leaked spallation neutron fluxes using low-energy proton projectiles are accessible using higher currents; meanwhile, this increases deposited heat inside the uranium targets. In contrast, irradiation of uranium target using high-energy proton could noticeably increase the neutron flux without much heating of the target. According to Fig. 15, application of 250-MeV proton energy increases the leaked spallation neutron yield up to 130 times than the one produced by 30-MeV protons. Meanwhile, the deposited heat becomes 10 times than the investigated 30 MeV energy.

However, absorption cross sections of natural uranium target in fast and epithermal neutron energy are noticeably

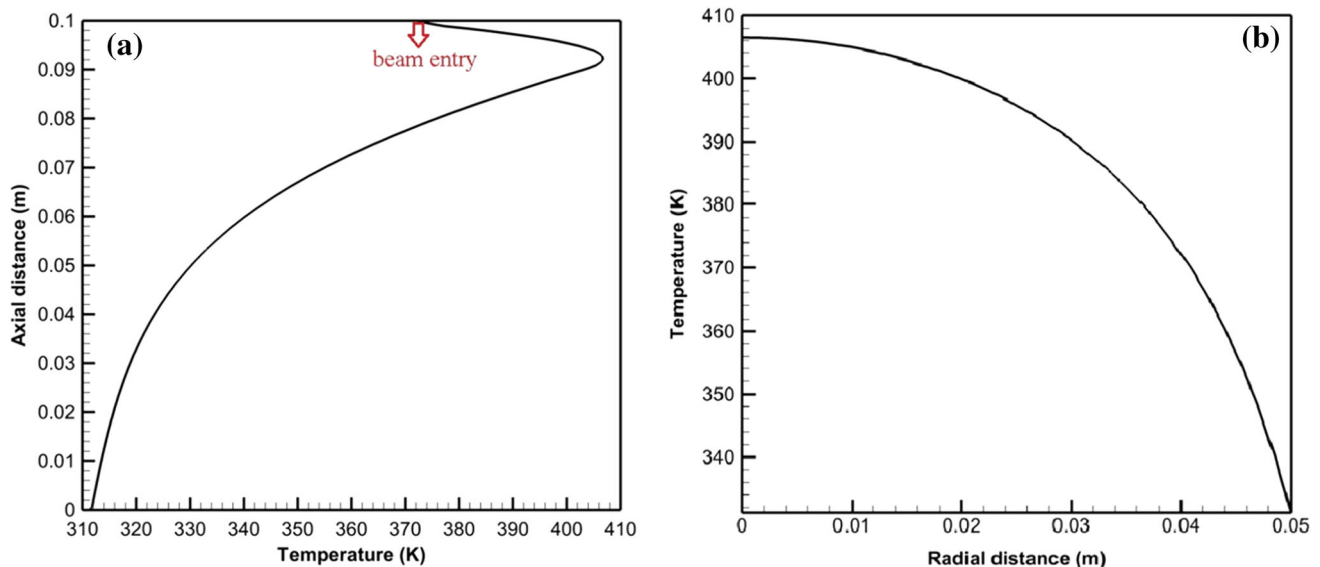


**Fig. 14** Temperature distribution inside the irradiated uranium target **a** axial, **b** radial ( $z = 0.09$ , the hottest plane)

**Table 3** Investigation of the produced neutrons by different reactions inside the  $10 \times 10$  cm cylindrical target irradiated by 30-MeV protons

Target situation	Escaped neutron yield	INC	$(p, f)$	$(n, f)$	$(n, f)$ by $2 < E_n < 30$ MeV	$(n, nx)$
Bare	0.036364	0.03367	0.00080	0.00371	0.00275	0.00050
Water-cooled	0.083563	0.03368	0.00085	0.01270	0.00275	0.00050

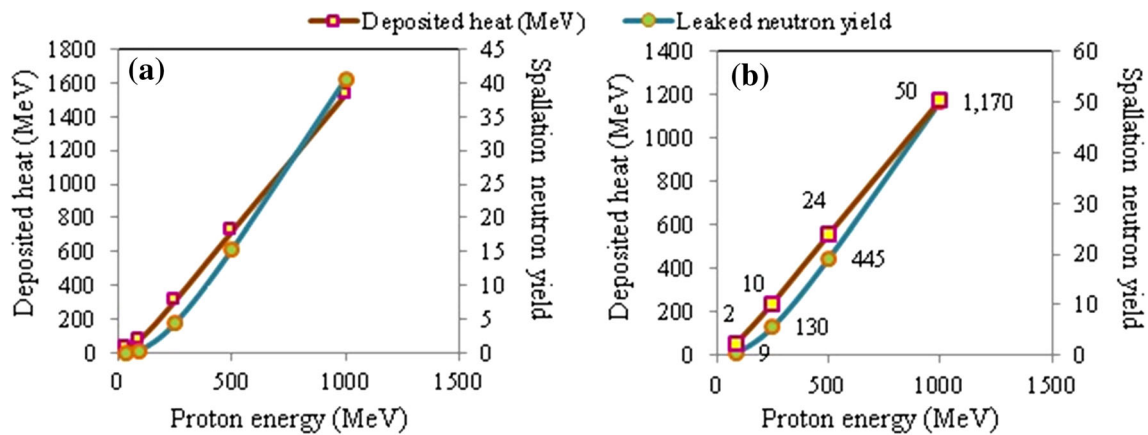


**Fig. 15** High-energy proton impacts on leaked neutron yield and deposited heat, uranium target dimension:  $5 \times 50$  cm, **a** direct values, **b** multiplied values in comparison with the target irradiated by 30 MeV

higher than other costmary spallation targets such as lead, lead–bismuth, mercury–tungsten, but its high fission cross sections compensate the drawback by creating a neutron yield of 3–4 times in comparison with the other targets using the same projectile energy and target dimension.

Overall, an accelerator-based neutron source produces pulsed neutron beams, which could be cost-effective in comparison with high efficiency reactor-based neutron sources that produce steady higher flux neutron beams. However, an accelerator-based one produces pulsed lower flux neutron beams, but proliferation resistance issues and safety operation that comes with nuclear reactors make a growing interest on construction of accelerator-based neutron sources. In addition, these accelerator-based neutron sources have low background between pulses and thereby good signal-to-noise ratio. Electron particles could be applied to generate neutrons in a heavy target by  $(\gamma, n)$  reactions. Nevertheless, only very high-energy electrons could produce suitable neutron yield and it is reported a 100-MeV  $e^-$  on  $^{238}\text{U}$  produces a neutron flux in order of  $3.1 \times 10^{15}$  n/MW, while 800-MeV  $p$  on  $^{238}\text{U}$  could produce a neutron flux in order of  $1.1 \times 10^{17}$  n/MW [19–21]. In case of our investigated neutron source, the produced neutron flux is in order of  $\sim 10^9$  n/MW using injection of 30-MeV proton beam of 100  $\mu\text{A}$  current in the optimized natural uranium target.

In addition, other low-energy accelerator-based methods were investigated to produce an external neutron source. Miyamaru et al. [22] evaluated the neutron emission profile of the  $^9\text{Be}(d, n)^{10}\text{B}$  nuclear reaction using a low-energy deuteron beam (300 keV) to develop an accelerator neutron source. Their results show the system is able to produce a neutron flux in order of  $10^{10}$  n/s  $\text{cm}^2$  in the utilized heavy water moderator using 50 mA current. Therefore, the source produces  $\sim 66 \times 10^{10}$  n/MW [22].

Capoulat et al. (2013) reported the medical application of a neutron field produced by bombarding a thin Be target (8  $\mu\text{m}$ ) with a 30-mA beam of 1.45-MeV deuterons [23].

Inada et al. [24] measured the energy and angular distributions as well as the yields of fast neutrons from a thick Be disk bombarded by 1.0- to 3.0-MeV deuterons. Their obtained results showed about  $5.6 \times 10^5$  n/MW could be available using 2.3-MeV deuterons induced on Be target.

Logan et al. [25] designed a compact beryllium target which produces a neutron flux of about  $6 \times 10^7$  n/MW ( $E > 1$  MeV) when bombarded with 20  $\mu\text{A}$  of 30-MeV deuterons.

Overall, the study shows good potential of the 30-MeV proton cyclotrons (CYCLONE30) for production of an external neutron source with acceptable intensity for many research aims. Nevertheless, the calculations were carried out based on the estimation of the threshold energy for spallation induction on  $^{nat}\text{U}$  target, which meets the rough estimation of particle wavelength and nuclear radius. It should be noted that the assurance for accurate application of the INC model for such low-energy calculations needs benchmarked or experimental validations.

A few experimental and benchmark studies have been done to determine validity of INC models at low-projectile energies. Thanks for David's valuable study [26], which focused on a review of spallation reactions as a successful interplay between modeling and applications. The work reported a comparison of INCL4.5 and INCL4.6 predictions for the neutron double differential cross sections in  $p(63 \text{ MeV}) + \text{Pb}$  collisions, which shows a good conformity with experimental data. In addition, the model is in good conventionality in the case of  $^9\text{Be}(d, xn)$  for 18-MeV projectile. Another investigation on  $p(175 \text{ MeV}) + \text{Ni}$  reported by David indicates both Isabel and INCL4.5 plus Abla de-excitation models present acceptable agreements

with the experimental. As the data reported by David, mass distributions of the nuclide production given by INCL4 and Isabel models for the reaction  $^{56}\text{Fe} (300\text{A} \cdot \text{MeV}) + \text{p}$  have good agreements with the available experimental.

Another work carried out by Blann et al. [27] shows there is about 7 % relative discrepancy between neutron multiplication calculated by Bertini + pre-equilibrium model and the experimental data of  $\text{p}(80 \text{ MeV}) + \text{Pb}$ , and about 15 % relative discrepancy between the other presented multiplications and Isabel + pre-equilibrium model. In addition, at that time they reported there is room for improvement in all codes, and that modeling calculations on a predictive basis may have uncertainties of the order of  $\pm 50$  %. However, the available INC models of the different computational codes improved much until now, but there maybe are many blanks to validate utilization of such codes for low-energy INC calculations.

## 4 Conclusion

Spallation targets can be applied to produce an external source of neutrons, which are wildly used for radioisotope production, neutron radiography or neutron therapy. Computational codes could efficiently be used to predict neutronic and thermal hydraulic performance of a spallation target. The present study illustrates that there is no noticeable relative discrepancy between different physical models for calculation of spallation neutron yield and deposited heat values in uranium target irradiated by 30- to 90-MeV protons. Light water at 1 atm pressure could easily cool the  $10 \times 10$  cm cylindrical uranium target irradiated by 30-MeV protons of 100  $\mu\text{A}$  current. The spallation target produces a leaked neutron flux in order of  $10^7$  n/s  $\text{cm}^2$ . Obviously, higher neutron fluxes using low-energy protons could be obtained by higher proton current registration inside the spallation target, but it would increase the deposited power. The mentioned problem confronts the system to metal coolant need or light water coolant usage at higher pressures. However, higher proton energies seem to be more capable of inducing the spallation process in uranium targets, but shielding challenges of such neutron source systems should be considered as major concerns.

## References

- G.J. Russell, *Spallation Physics—An Overview*. ICANS-XI International Collaboration on Advanced Neutron Sources KEK. Tsukuba, 22–26 Oct 1990
- K. Ismailov, M. Saito, H. Sagara et al., Feasibility of uranium spallation target in accelerator-driven system. *Prog. Nucl. Energy* **53**, 925–929 (2011). doi:10.1016/j.pnucene.2011.05.019
- S.R. Hashemi-Nezhad, I. Zhuk, M. Kievets et al., Determination of natural uranium fission rate in fast spallation and fission neutron field: an experimental and Monte Carlo study. *Nucl. Instrum. Methods Phys. Res. A* **591**, 517–529 (2008). doi:10.1016/j.nima.2008.02.101
- S.R. Hashemi-Nezhad, W. Westmeier, M. Zamani-Valasiadou et al., Optimal ion beam, target type and size for accelerator driven systems: implications to the associated accelerator power. *Ann. Nucl. Energy* **38**, 1144–1155 (2011). doi:10.1016/j.anucene.2010.12.008
- S. Sahin, B. Sarer, Y. Celik, Energy multiplication and fissile fuel breeding limits of accelerator-driven systems with uranium and thorium targets. *Int. J. Hydrogen Energy* **40**, 4037–4046 (2015). doi:10.1016/j.ijhydene.2015.01.141
- G.J. Russell, J.S. Gilmore, S.D. Prael et al., Los Alamos Scientific Lab., NM (USA); Kansas State Univ., Manhattan (USA) Spallation target-moderator-reflector studies at the Weapons Neutron Research. 1980; 26 p; Symposium on neutron cross sections from 10–50 MeV. Upton, NY, USA, 12–14 May 1980
- R.G. Vasil'kov, V.I. Gol'danskij, B.A. Pimenov et al., Neutron multiplication in uranium bombarded with 300–660 MeV protons. *Sov. J. At. Energy* **44**(4), 329–335 (1978)
- D.B. Pelowitz, *Users' manual versión of MCNPX2.6.0*, LANL, LA-CP-07-1473 (2008)
- A. Krása, in *Spallation Reaction Physics*, this is a revised version of the manuscript for the lecture\Neutron Sources for ADS for students of the Faculty of Nuclear Sciences and Physical Engineering at Czech Technical University in Prague, May 2010
- W.M. Stacy, *Nuclear Reactor Physics* (Wiley, Hoboken, 2001)
- M.J. Kim, H. Bhang, J.H. Kim et al., A Monte-Carlo intranuclear cascade calculation for the propagation of energetic neutrons in the nucleus. *J. Korean Phys. Soc.* **46**(4), 805–812 (2005)
- J.K. Shultis, R.E. Faw, *An MCNP Primer*. Dept. of Mechanical and Nuclear Engineering, Kansas State University. Copyright: 2004–2010
- J.F. Briesmeister, *MCNP-A General Monte Carlo N-Particle Transport code Version 4C*. Los Alamos National Laboratory Report, USA, LA-13709-M (2000)
- D. Ridikas, *Radioactivity Inventory of the Test Uranium Target at TRIUMF*. Internal report: CEA Saclay, DSM/IRFU/SPhN, March 2008
- B. Rapp, J.C. David, V. Blideanu, D. Doré et al., Benchmarking of the modeling tools within the EURISOL DS project, in *Proceedings of International Workshop on Shielding Aspects of Accelerators, Targets and Irradiation Facilities (SATIF-8)*, Pohang, South Korea, 22–26 May 2006
- A.W. Schulke Jr., IPNS enriched uranium booster target, in *Proceedings of the Eighth Meeting of the International Collaboration on Advanced Neutron Sources (ICANS-VIII)*, Rutherford Appleton Laboratory Report RAL-85-110. 8–12 July 1985
- K.D. Timmerhaus, R.W. Fast, A.F. Clark et al., *Adv. Cryog. Eng.* **31**, 1017 (1985)
- Y. Malyshkin, I. Pshenichnov, I. Mishustin et al., Monte Carlo modeling of spallation targets containing uranium and americium. *Nucl. Instrum. Methods Phys. Res. B* **334**, 8–17 (2014)
- W. Chou, *Spallation Neutron Sources and Other High Intensity Proton Sources* (Fermi National Accelerator Laboratory, Batavia, 2003)
- R. Pynn, in *Spallation Neutron Source & Neutron Production* (Indiana University, Bloomington)
- S.C. Joshi, *Critical Aspects of Spallation Neutron Sources*. Raja Ramanna Centre for Advanced Technology, Indorem Indo-Japan School on Advanced Accelerators of Ions & Electrons, 17 Feb 2015
- H. Miyamaru, I. Murata, Y. Ootera et al., Neutron emission profile of d-Be reaction with low-energy deuteron beam for accelerator neutron source. *J. Nucl. Sci. Technol.* **5**, 58–61 (2008)

23. M.E. Capoulat, M.S. Herrera, D.M. Minsky et al., The  $9\text{Be}(d,n)$   $1\text{B}$  reaction as a neutron source for boron neutron capture therapy, in *X Latin American Symposium on Nuclear Physics and Applications (X LASNPA)*, 1–6 December, Montevideo, Uruguay (2013)
24. T. Inada, K. Kawachi, T. Hiramoto, Neutrons from thick target beryllium (d,n) reactions at 1.0 MeV to 3.0 MeV. *J. Nucl. Sci. Technol.* **5**, 22–29 (1968)
25. C.M. Logan, R. Booth, R. Nickerson, A compact berkelium target for production of fast neutrons. *Nucl. Instrum. Methods* **145**, 77–79 (1977)
26. J.C. David, Spallation reactions: a successful interplay between modeling and applications. *Eur. Phys. J. A* **51**, 1–57 (2015)
27. M. Blann, H. Gruppelaar, P. Nagel et al., International code comparison for intermediate energy, in *Nuclear Energy Agency Organization for Economic Co-operation and Development* (1993)